

tAF-MUSICAL: Autofluorescence Super-resolution Microscopy for Molecular Histopathology of Matrix Proteins in Fibrotic Diseases

Biswajoy Ghosh,¹ Jyotirmoy Chatterjee,¹ Ranjan Rashmi Paul,² Pooja Lahiri,¹ Mousumi Pal,² Pabitra Mitra,¹ Balpreet Singh Ahluwalia,^{3,4} Krishna Agarwal,^{3*}

¹Indian Institute of Technology Kharagpur, West Bengal, India

²Guru Nanak Institute of Dental Sciences and Research, Kolkata, West Bengal, India

³UiT - The Arctic University of Norway, Tromsø, Norway

⁴Department of Clinical Science, Intervention and Technology,
Karolinska Institute, Stockholm, Sweden

*To whom correspondence should be addressed; E-mail: krishna.agarwal@uit.no.

Supplementary Information

Supplementary Figs. S1 to S11

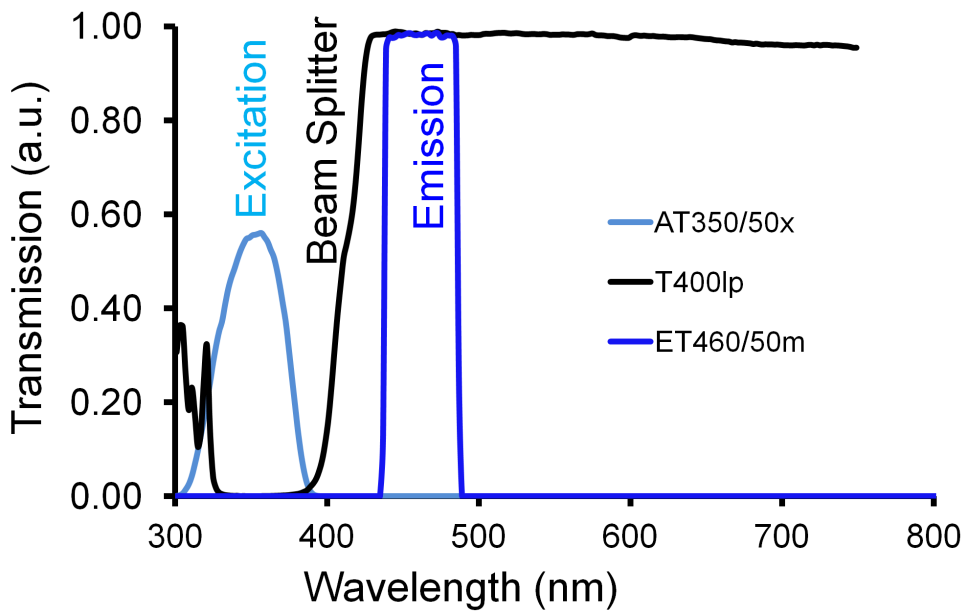


Figure S1: Fluorescence spectra for tAF-MUSICAL of matrix proteins. Figure shows the fluorescence filter's spectral characteristics for capturing the matrix proteins—collagen and keratin from tissue sections. The optical filter-set of epifluorescence microscope uses a $\bar{\lambda}_{ex}=350$ nm, $\Delta\lambda=100$ nm for excitation and a $\bar{\lambda}_{em}=460$ nm, $\Delta\lambda=100$ nm. A long pass filter beyond 400 nm is used as a beam splitter.

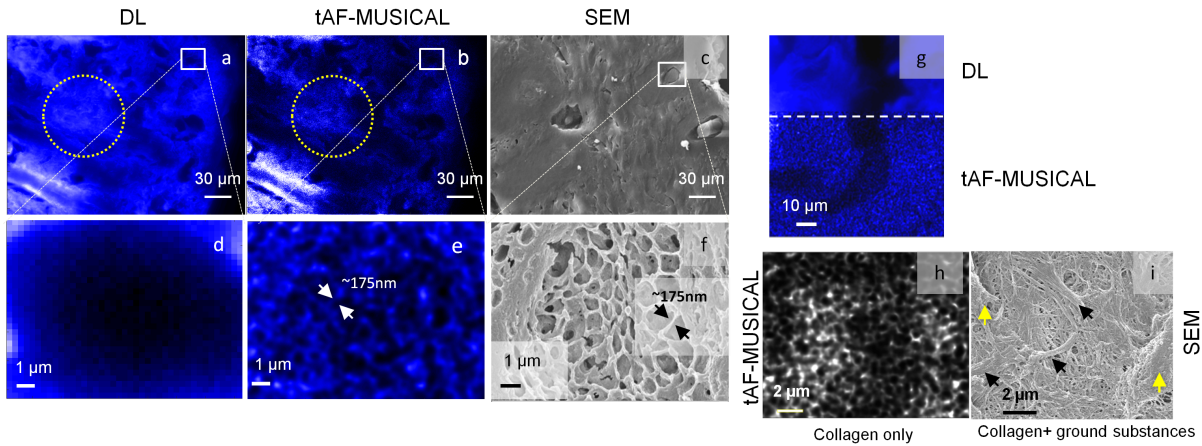


Figure S2: Performance of tAF MUSICAL to visualize collagen fibers. (a,b) are the diffraction-limited (DL) and tAF-MUSICAL image of the same region of the mice skin tissue. (c) SEM image of the same skin tissue taken in the same region (not spatially matched). The dotted circles in (a) and (b) shows enhancement of collagen density variations by tAF-MUSICAL, (d,e,f) shows a small ROI of the three images zoomed in from a,b, and c at a skin follicle region, (g) visualizes the resolution improvement of tAF-MUSICAL from the diffraction-limited image taken at $20\times$ magnification with 0.4 NA objective. (h,i) compares the tAF-MUSICAL and SEM, illustrating that in tAF-MUSICAL images the fibrous collagen mesh selectively images collagen fibrils while SEM images present collagen fibers (black arrows) as well as non-fibrous extracellular matrix components (yellow arrows) that often mask the fibers, thereby restricting visualization.

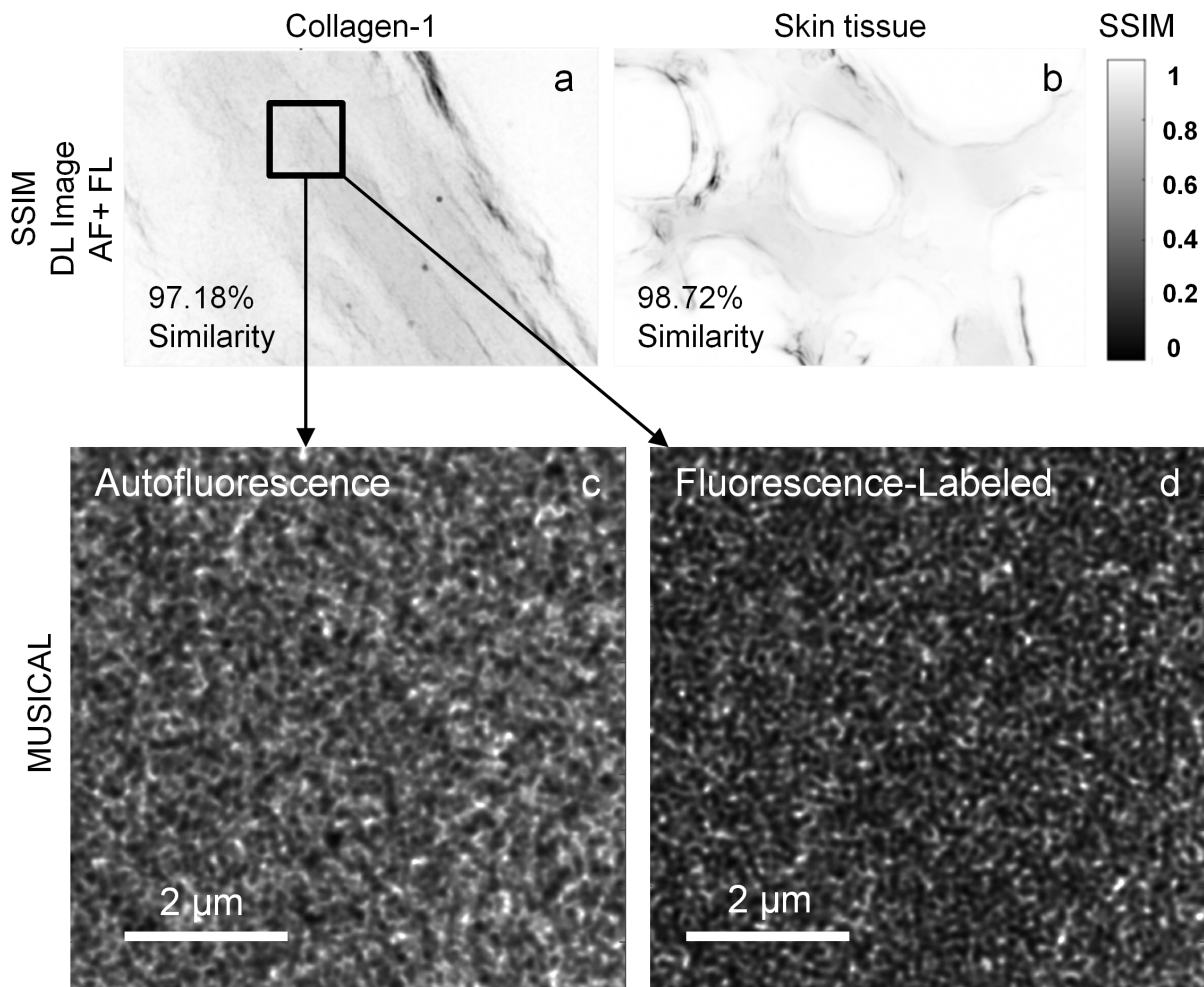


Figure S3: Structural similarity analysis of autofluorescence and tagged-fluorescence of MUSICAL. (a,b,c,d) overlaid collagen-I autofluorescence (blue) and collagen labeled (red) images in large field and ROI. (e,f,g,h) structural similarity measure (SSIM map) between autofluorescence and tagged-fluorescence. The similarity scores between the autofluorescence and labeled fluorescence when super-resolved by MUSICAL are 66-69%. (i,j) the similarity maps between tissue autofluorescence and labeled fluorescence for collagen-I and tissue with diffraction-limited imaging. The similarity scores are 97.18% and 98.72%.

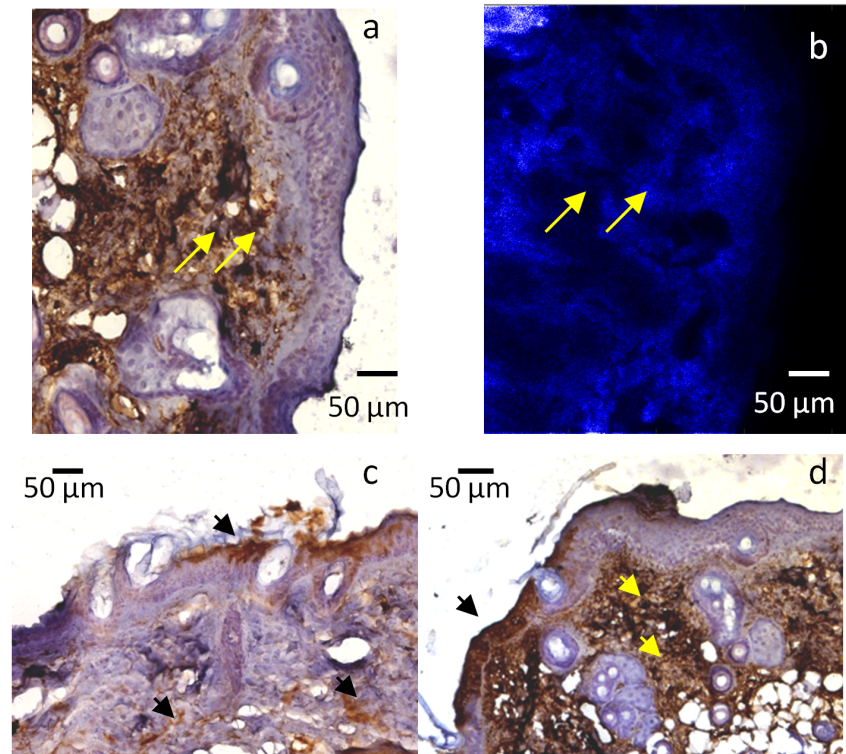


Figure S4: Comparison of collagen immuno-staining with tAF-MUSICAL. (a,b) collagen-I immuno-labeled tissue section and corresponding tAF-MUSICAL from the same tissue section and same location (not spatially matched). The yellow arrows show over-staining that inaccurately indicate higher collagen densities, causing subjectivity. (c,d) shows the most commonly occurring issues with collagen immuno-labeling i.e., non-uniform collagen staining wherein (c) shows under-staining, and (d) shows over-staining. The black arrows highlight unspecific staining (black arrows shows stain uptake in the epithelium, which does not contain collagen).

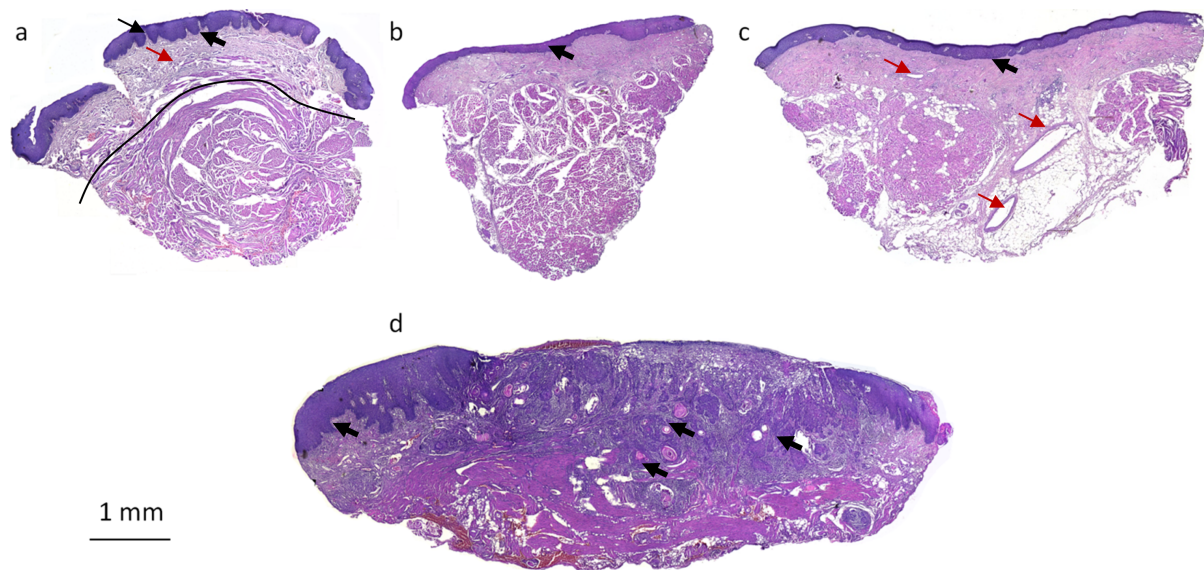


Figure S5: Histology of representative full oral tissues sections with varying levels of pathology associated with oral carcinoma. (a) Hematoxylin and eosin (HE) stain of the normal oral mucosa (NOM), the darker stained outer epithelium (black arrows), and sub-epithelium (red arrow). The region below the black line is majorly muscle tissues; the bold black arrow shows the epithelium's rete pegs, i.e., undulations at the base of the epithelial layer. (b) HE of oral submucous fibrosis (OSF) shows denser epithelium and flattened rete pegs (bold arrow). (c)HE of oral submucous fibrosis with dysplasia (OSFD,) with flattened rete pegs (bold arrow), dense sub-epithelium, and perivascular fibrosis (red arrows). (m) HE of oral squamous cell carcinoma (OSCC), with the epithelial basement membrane, lost continuity and invaded into subepithelium (bold arrows).

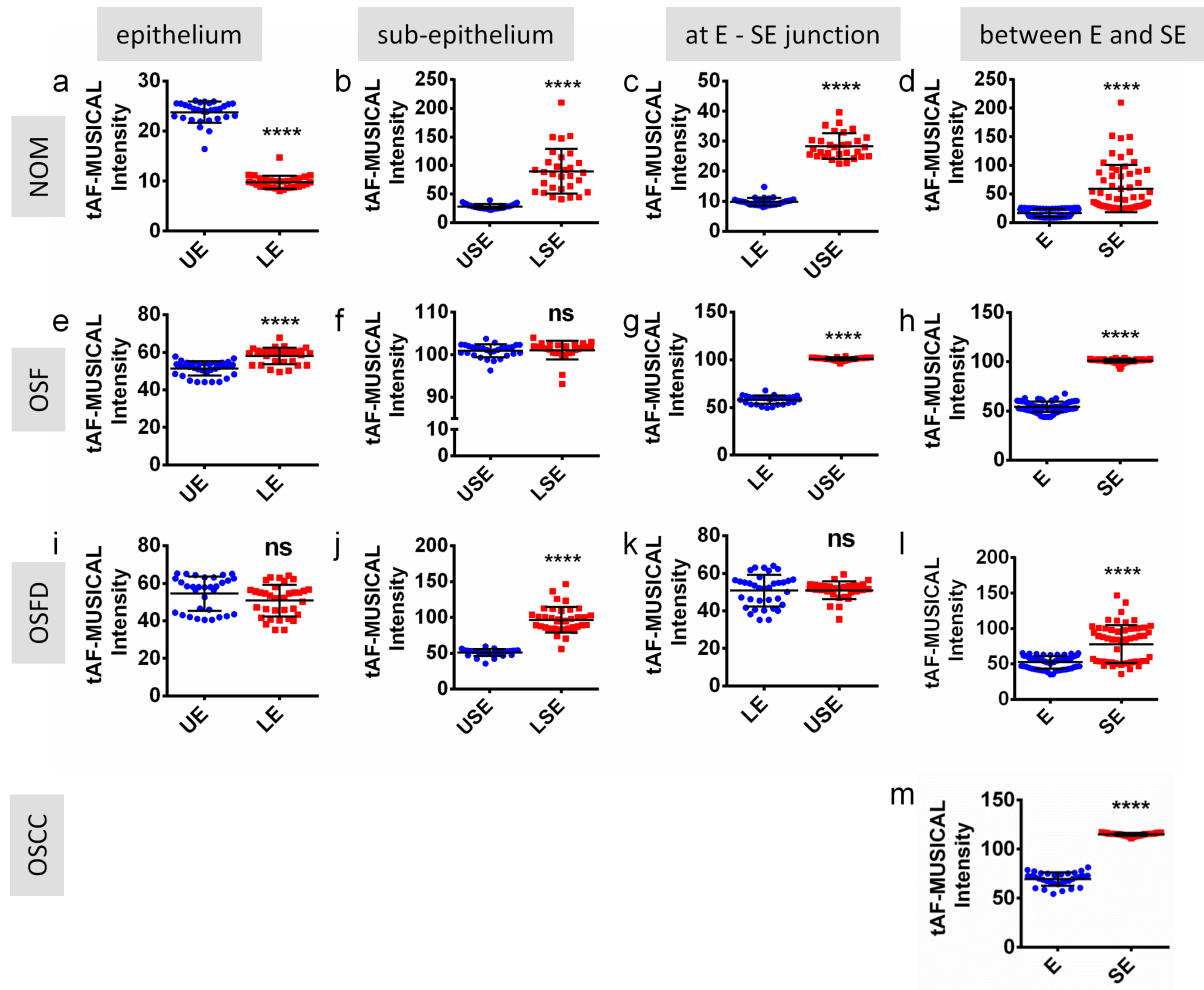


Figure S6: Quantification of collagen intensities from tAF-MUSICAL images in oral pre-cancer and cancer tissues. The difference of tAF-MUSICAL intensities at different tissue layers of oral submucous fibrosis including (a-d) normal oral mucosa (NOM), (e-h) oral submucous fibrosis (OSF), (i-l) oral submucous fibrosis with dysplasia (OSFD), and (m) oral squamous cell carcinoma (OSCC), differences between epithelial and subepithelial layers is not possible in invasive cancer due to loss of tissue integrity. Therefore the epithelial and subepithelial islands have been considered for comparison. UE—upper epithelium, LE—lower epithelium, USE—upper sub-epithelium, LSE—lower sub-epithelium.

Note: UE, LE, USE, LSE of tAF-MUSICAL histologically represent epithelium proper, basal/suprabasal epithelium, papillary sub-epithelium and reticular sub-epithelium respectively.

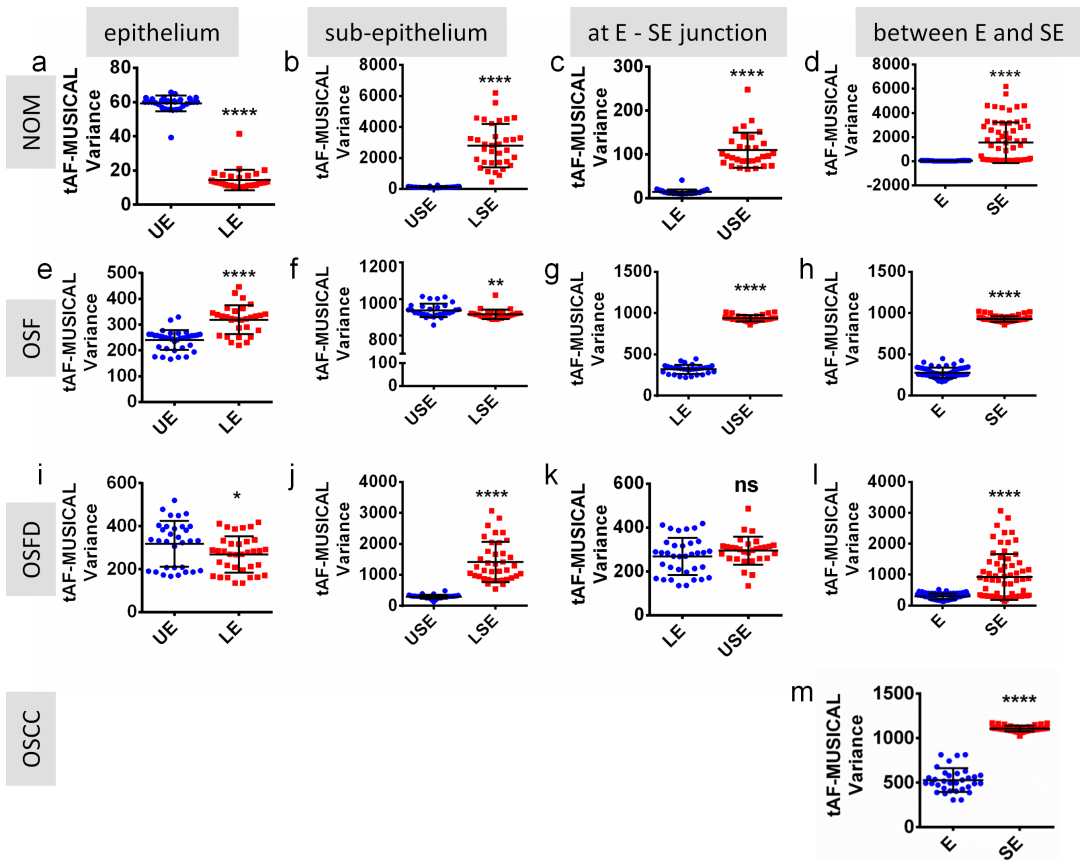


Figure S7: Quantification of collagen variance from tAF-MUSICAL images in oral pre-cancer and cancer tissues. The difference of tAF-MUSICAL variance at different tissue layers of oral submucous fibrosis including (a-d) normal oral mucosa (NOM), (e-h) oral submucous fibrosis (OSF) (i-l) oral submucous fibrosis with dysplasia (OSFD) and (m) oral squamous cell carcinoma (OSCC), differences between epithelial and subepithelial layers is not possible in invasive cancer due to loss of tissue integrity. Therefore the epithelial and subepithelial islands have been considered for comparison. *E*—epithelium whole, *UE*—upper epithelium, *LE*—lower epithelium, *SE*—sub-epithelium whole, *USE*—upper sub-epithelium, *LSE*—lower sub-epithelium.

Note: *UE, LE, USE, LSE* of tAF-MUSICAL histologically represent epithelium proper, basal/suprabasal epithelium, papillary sub-epithelium and reticular sub-epithelium respectively.

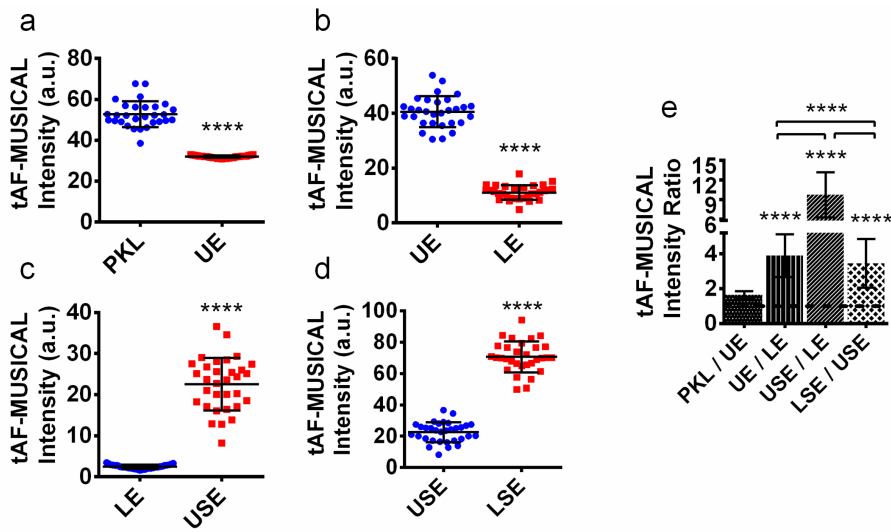


Figure S8: Quantification of matrix variations from tAF-MUSICAL images in oral epithelium with Leukoplakia. tAF-MUSICAL intensities between the (a) epithelial layers —PKL and UE (b) the epithelial layers —UE and LE, (c) the epithelial layer—LE and the sub-epithelial layer—USE (d) the sub-epithelial layers—USE and LSE. (e) The ratio of tAF-MUSICAL intensities between subsequent layers across an oral Leukoplakia tissue. (f) the intensity of pan-keratin stain in the epithelial layers —PKL, UE, and LE, (g) Ratio of immunolabeled pan-keratin stain intensities between subsequent layers across an oral Leukoplakia tissue. *PKL*—para keratinized layer, *UE*—upper epithelium, *LE*—lower epithelium, *USE*—upper sub-epithelium, *LSE*—lower sub-epithelium.

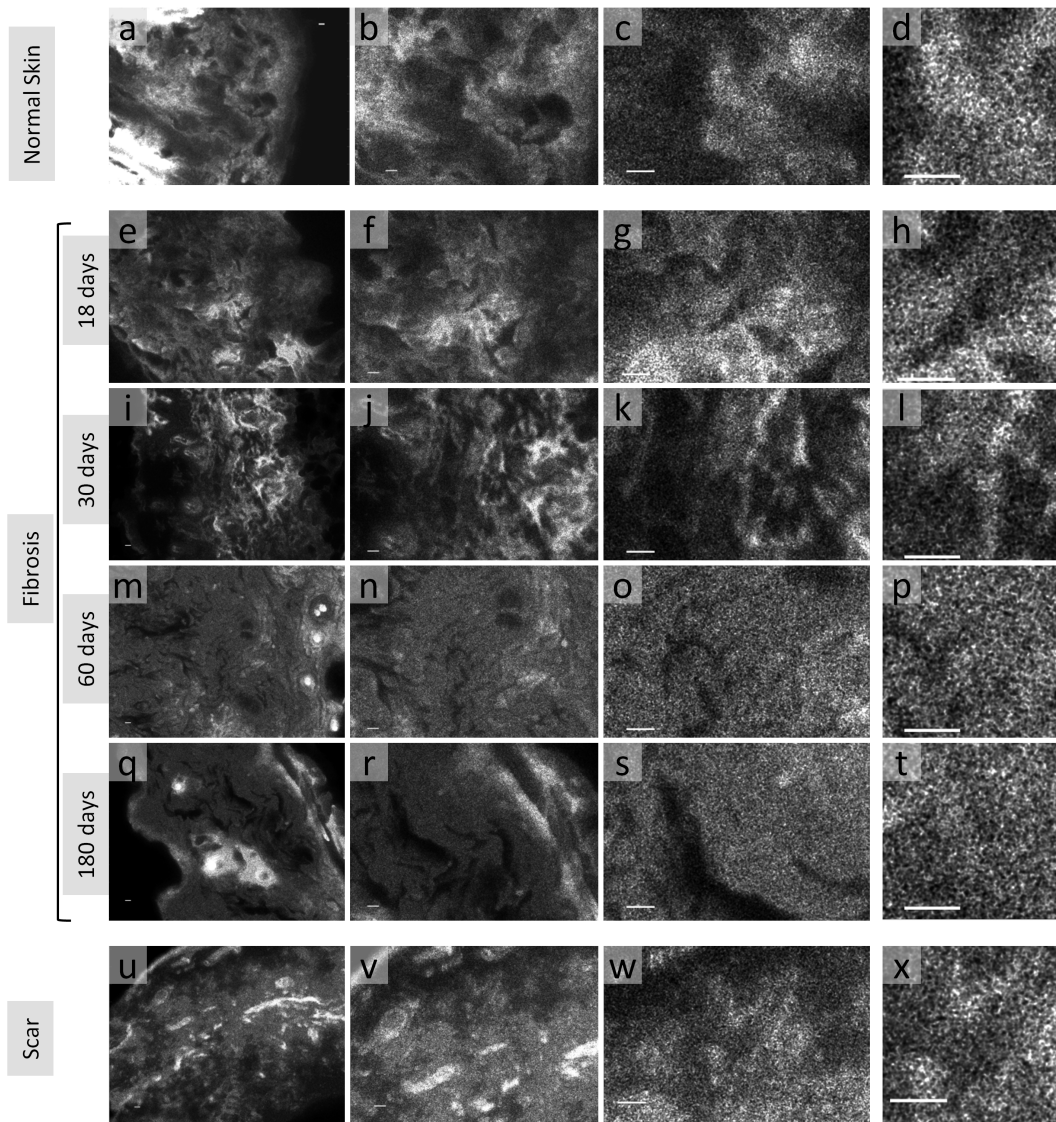


Figure S9: Multi-scale tAF-MUSICAL images of healthy and fibrotic skin tissues. (a-d) tAF-MUSICAL images of a healthy skin tissue visualized at image sizes of (a) 10000×13400 (full field of view), (b) 4000×5000 , (c) 2000×3000 , and (d) 1000×1000 . The four image dimensions have been illustrated for progressive pathological fibrosis at (e-h) 18 days, (i-l) 30 days, (m-p) 60 days, and (q-t) 180 days; here, while 18 days and 30 days treatment are early fibrosis, 60 days and 180 days are advanced fibrosis. (u-t) images of scar tissue collected from 60 days of wound healing at the same dimensions as healthy skin. *scale bar= 2 μ m.*

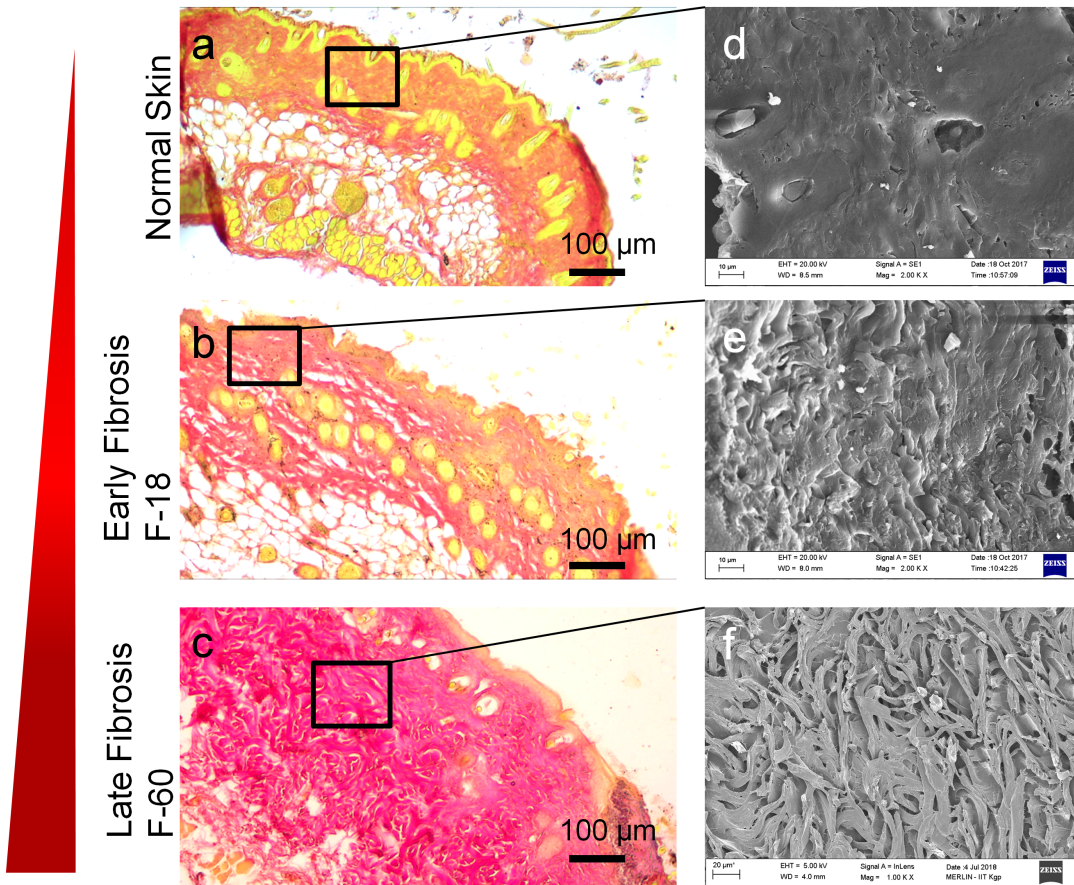


Figure S10: Histology and SEM of arecanut-induced fibrosis in mice skin. (a-c) VG stained images of normal skin, and fibrosis upon arecanut treatment on 18 days (represent early fibrosis) and 60 days (represent late fibrosis). With the advancement of fibrosis the red color (indicating collagen) becomes more prominent and the yellow reduces indicating loss of non-fibrosis ECM or ground substance. (d-f) SEM of the corresponding stages of fibrosis. It can be seen with advancement of fibrosis the image acquires a rough texture. In late fibrosis thick collagen bundles can be clearly observed, while they are least discernible in the normal skin.

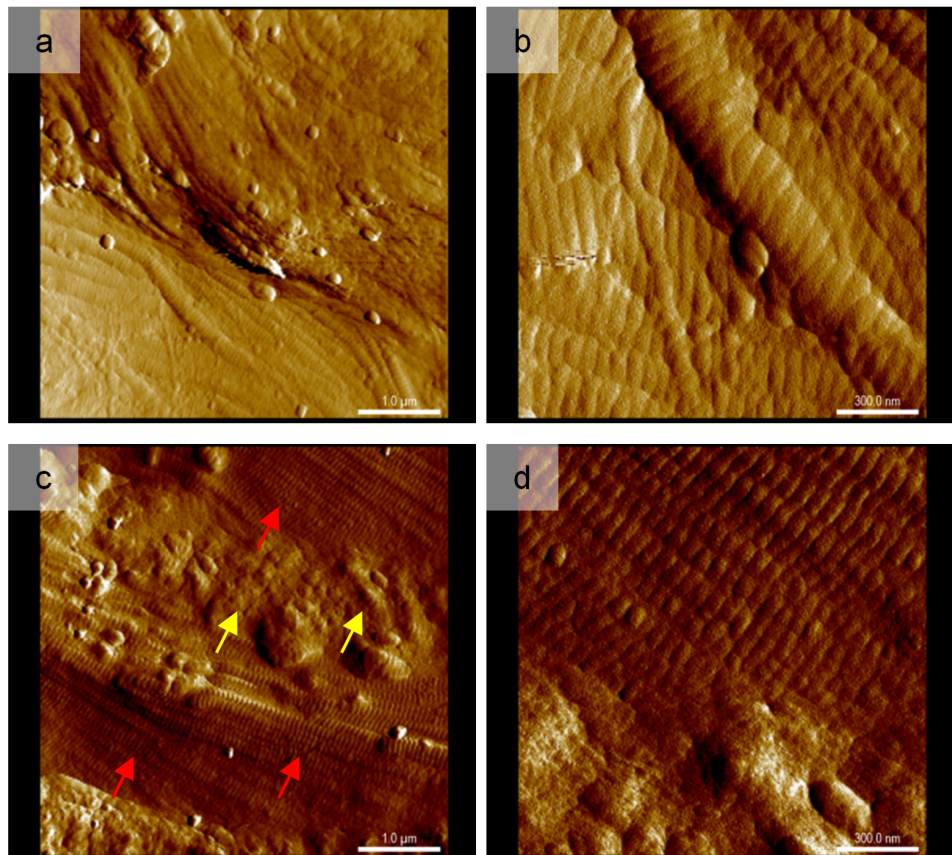


Figure S11: Collagen ultra-structure in healthy and fibrotic skin tissue. (a) AFM image of collagen fibrils of a healthy mouse skin tissue and (b) higher resolution picture depicting variation in fibril thickness in healthy tissue, (c) AFM image of collagen fibrils of a fibrotic (scar, after 60 days of wound healing) mouse skin tissue, the red arrows point to collagen fibrils while the yellow arrows point to the non-fibrous extracellular matrix (d) higher resolution picture depicting uniformity in fibril thickness in the scar tissue.